JOURNAL of QASSIM UNIVERSITY FOR SCIENCE
© 2022 Qassim University [E-ISSN: 1658-9610]
Vol. 1, Issue 1, pp 129-153 (October 2022)
JQUS

Synthesis, spectroscopic, and antibacterial studies of new Schiff-base and organophosphorus Schiff-base with some transition metal (II) ions

Yasmin M.S. Jamil[*1], Fathi M. Al-Azab[1], Nedhal A. A. Al-Selwi[1] , Fatima M. M. Al-duais[1], Ahmed N. Al-Hakimi[2,3], Ibrahim A. Alhagri[2,3], S. El-Sayed Saeed[2]

[1]Department of Chemistry, Faculty of Science, Sana'a University, Yemen
[2] Department of Chemistry, College of Science, Qassim University, Buraidah-51452, Saudi Arabia.
[3] Department of Chemistry, College of Science, Ibb University, Ibb, Yemen.

*Corresponding author: y.jamil@su.edu.ye, yasminjml@yahoo.com

Abstract

A new transition metal complexes of Cu (II), Co (II) , and Ni (II) were synthesized from the Schiff base (2-Furalidene-1-phenylsemicarbazide **SB**) and the organophosphorus Schiff base (2-Furalidenediphenylphosphate-1-phenylsemicarbazide **OPSB**). The ligands were characterized from their metal analysis, IR, UV-Vis, NMR, and XRD spectral studies. The structural features of complexes were obtained by their elemental analyses, magnetic susceptibility, molar conductance, IR, UV-Vis spectral, and molar ratio studies. The data showed that these complexes have the composition of ML_2 for **SB** ligand and ML for **OPSB.** According to the UV-Vis, magnetic susceptibility data the octahedral geometry was suggested for all complexes. From XRD results, the practical size of ligands and SB complexes were in the nano range with crystallinity structure. The ligands and their metal complexes have been screened for their antioxidant, antibacterial and antifungal activity.

Keywords: Schiff base, organophosphorus Schiff base, XRD; antioxidant.

1. Introduction

Schiff bases are compounds characterized by the azomethine group (>C=N–), as described by Hugo Schiff in 1864 [1]. The Schiff base compounds are commonly used as ligands in the synthesis of coordination compounds. These compounds have an important role due to their physiological and pharmaceutical activities [2]. In biological chemistry, Schiff bases have elucidation a wide range of biological activities, including an antifungal, antibacterial, antiviral and recently anticancer effect that has been provided [3-6]. A survey of the literature reveals a work devoted to the synthesis, characterization, and biological activities of many metal complexes of Schiff base from 2-Furaldehyde [7-11]. Furthermore, the coordination of organophosphorus compounds with transition metal ions has been the subject of several studies since complexes of such compounds exhibit biological activity [12-16]. This paper explain the preparation and characterization of Schiff base of 2-Furaldehyde with 1-phenylsemicarbazide and organophosphorus Schiff base followed by studying their complexation with transition metal ions which have been the subject of several studies because these ligands and their metal complexes exhibit different biological activity.

2. Experimental

2.1. Materials

A high purity chemicals were used from many companies. These chemicals were listed in Table 1:

Table1: The used chemicals

Substance	Company
1-phenylsemicarbazide ($C_7H_9N_3O$)	Riedel-dehaen
2-Furaldehyde (Furfural) ($C_5H_4O_2$)	Aldrich
Diphenyl Chlorophosphat ($C_{10}H_{12}PO_2Cl$	Riedel-dehaen
Copper chloride dihydrate ($CuCl_2.2H_2O$)	Riedel-dehaen
Nickel chloride hexahydrate ($NiCl_2.6H_2O$)	BDH
Cobalt chloride hexahydrate ($CoCl_2.6H_2O$)	BDH
Triethyl amine ($C_6H_{15}N$)	BDH
Ferric chloride ($FeCl_3$)	BDH
Bipyridine ($C_{10}H_8N_2$)	Aldrich
Ascorbic acid ($C_6H_8O_6$)	BDH
Sodium acetate trihydrate ($C_2H_9NaO_5$)	BDH
Glacial acetic acid ($C_2H_4O_2$)	BDH
Solvents	BDH, Aldrich

2.2. Preparation of ligands

At the beginning, the Schiff base (SB) was prepared by condensation between an ethanolic solution of amine (1-phenylsemicarbazide) (7.55g, 0.05 mole) with an ethanolic solution of aldehyde (2-Furaldehyde) (4.80g, 0.05 mole) (Scheme 1). The product separated out on cooling. It was filtered, washed several times with ethanol, ether, then recrystallized by ethanol to give the corresponding Schiff base. Secondly, the organophosphorus Schiff base (OPSB) was prepared by condensation between a

solution of Schiff base (3.43g, 0.015 mole) in dry benzene (50 ml) with a solution of diphenyl chlorophosphate (3.69g, 0.015 mole) in dry benzene (50 ml) in 1:1 molar ratio in presence of triethyl amine (Scheme 2). After complete addition, the reaction mixture was heated under reflux for 2h. The formed solid (triethyl amine hydrochloride) was filtered and the product was obtained after evaporation on a water bath.

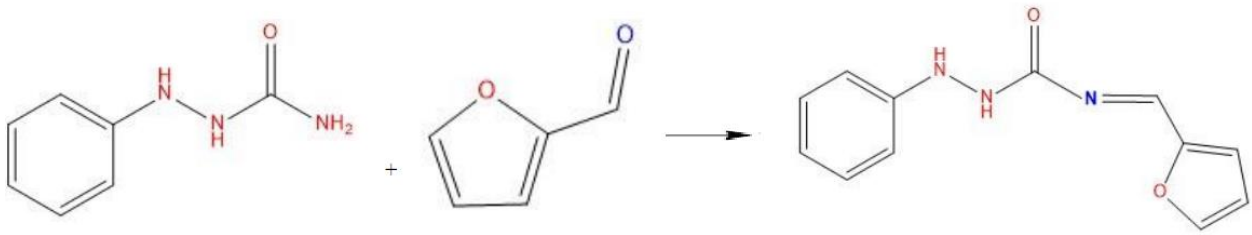

1-phenylsemicarbazide 2-Furaldehyde

Scheme 1: Preparation of base 2-furalidene-1-phenylsemicarbazide

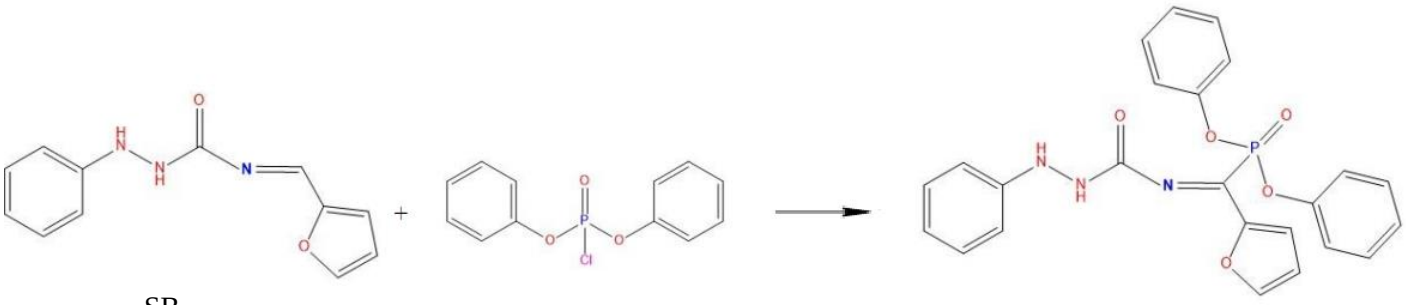

SB diphenylchlorophosphate

Scheme 2: Preparation of organophosphorus Schiff base 2-furalidenediphenylphosphate-1-phenylsemicarbazide

2.3. Preparation of metal complexes

2.3.1. Preparation of Schiff-base metal complexes

A hot ethanolic solution of metal chloride was added dropwise to an ethanolic solution of Schiff base (2L:1M) molar ratio. The mixture was refluxed on a hot plate with stirring for 2–3h. After evaporation of the solvent, the solid product was washed several times with ethanol and dried over anhydrous $CaCl_2$.

2.3.2. Preparation of organophosphorus metal complexes

A solution of metal chloride in 20 ml absolute ethanol was added dropwise to the solution of organophosphorus Schiff base in warm absolute ethanol (1L:1M). After the addition, the mixture was heated under hot reflux for three hours. The solution was evaporated and the solid complexes were collected by using ether.

2.4. Physical measurements

The elemental C, H, N analysis was carried out using a Vario EL Fab. CHNP Nr, at Central Laboratory, Faculty of Science, Cairo University, Giza, Egypt. The metal

content was measured using Perkin-Elmer 2380 flame atomic absorption spectrophotometer [17] at the central lab of the Ministry of Oil, Sana'a - Yemen. The molar conductance (10-3M) of the metal complexes in DMF solvent was measured on Jenway conductivity meter model 4510. All the measurements were taken at room temperature on freshly prepared solutions by applying relation [18]:

$$\Lambda m = 1000 \times L / C$$

Where, L is the specific conductivities of solution, C is the concentration and Λm is the molar conductance.

The infrared spectra of the ligands and their complexes were performed on (FT/IR-140, Jasco, Japan) spectrophotometer with KBr disc (4000–400 cm^{-1}), at Sana'a University. The NMR spectra of ligands were performed at (varian FT-300 MHz spectrometer) in d_6-DMSO solvent using TMS as internal standard, at Cairo University, Giza, Egypt. UV–vis spectra were performed by (specord200, Analytilk Jena, Germany) in the range 200-900 nm, at Sana'a University. Magnetic susceptibilities measurements were measured using Gouy's method [19] by a magnetic susceptibility balance from Johnson Metthey and Sherwood model. The effective magnetic moment (μeff) values were obtained using the following equations (1, 2 and 3):

$$X_g = \frac{C_{Bal} L (R - R_0)}{10^9 M} \qquad (1)$$

Where, R_o=Reading of empty tube, L=Sample length (cm), M=Sample mass (gm), R=Reading for tube with sample, C_{Bal}=balance calibration constant = 2.086

$$X_M = X_g \, x \; M.Wt \qquad (2)$$

The values of X_M as calculated from equation (2) are corrected for the diamagnetism of the ligands using Pascal's constants then used in Curie's equation (3).

$$\mu_{eff} = 2.84 \sqrt{X_M \; x \quad T} \qquad (3)$$

Where T= t (°C) + 273

All melting points reported for the compounds are measured in glass capillary tubes in degrees Celsius. Chloride was determined gravimetrically by silver nitrate [17]. The amount of coordinated and uncoordinated water molecules was determined gravimetrically using the weight loss method [20]. The XRD patterns were obtained using XD-2 (Shimadzu ED-720) powder X-ray diffractometer at a voltage of 35 kV and a current of mA using CuK(α) radiation in the range of $5^o < 2\theta < 70^o$ at 1^o min^{-1} scanning rate and a wavelength 1.54056 A^o, at Yemen Geological Survey and Mineral Resources Board.

2.5. Determination of the stoichiometry of the formed complexes of molecular structure (Molar ratio method)

The molar ratio of complexes was described by Molar ratio method [21]. The concentrations of metal ions (Cu^{2+}, Ni^{2+} and Co^{2+}) were kept constant at (1×10^{-3} M) in methanol, and the concentration of ligands (SB and OPSB) were regularly varied in methanol. The absorbance of the prepared solutions was measured at a constant wavelength (λmax). The absorbance values were plotted versus the molar ratio [ligand] / [metal ion]. The intersections of the obtained straight lines indicate the molar ratio of the stable complexes.

2.6. Crystallinity and particle size from XRD

The percentage of crystallinity, XC (%) was calculated based on the integrated peak areas of the principal peaks [22]. The crystallinity of the complexes is calculated relative to the crystallinity of the ligands as a ratio:

$$\mathbf{XC\ (\%) = (A_{complex})/\ (A_{ligand})\ x\ 100}$$

where $A_{complex}$ and A_{ligand} are the areas under the principal peaks of the complex and ligand sample, respectively.

X-ray diffraction was also used to determine the average particle size (D) which was estimated by the Scherrer equation [23, 24]:

$$\mathbf{D = K\ \lambda\ /\ \beta\ \cos\theta}$$

where **K** is Scherrer constant and equals 0.94, λ is the X-ray wavelength of Cu-Kα radiations (1.5405 A^{o}), β is full width at half maximum (FWHM) and θ is Bragg diffraction angle in degrees.

2.7. Antioxidant activity

Free radical liquidation activity of the compounds has been studied using Ferric-bipyridine reducing capacity of total antioxidants (FBRC) [25]. The fixed reaction time and fixed state measurement method were used to find out the antioxidant activity of these compounds in methanol as a solvent. All spectrophotometric measurements were measured using UV-Vis Spectrophotometer (Specord200, Analytikjena, Germany) at Sana'a University.

2.8. Antimicrobial activity

The prepared ligands and their metal complexes were evaluated for their antimicrobial activity in the Laboratory of microbiology at Sana'a University. They germinated four types of Bacteria (*Staphylococcous aureus, Bacillus subtilis, Escherichia.Coli and Pseudomonas aeruginosa*) and one fungi (*Candida albicans*) on Nutrient agar and sabouraud agar solid media respectively. Using the filter paper disc method [26], it was prepared one concentration from each compound (1000µg/ml) in DMSO. Then added (100µl) from each prepared solution on a filter paper disk (Whatman No.l filter paper, 5 mm diameter) which contained the bacteria with agar solid media, all the Petri-dishes were put in an incubation period at 37 oC for 24 hour. Gentamicin 120 µg/ml was used as a reference substance for bacteria and Mycostatin 30 µg/ml for fungi. The results were registered by calculating the diameter of the inhibition zone (mm).

3. Results and discussion

The Schiff base ligand was prepared by the condensation of 1-phenylsemicarbazide with Furfural (SB) in the molar ratio 1:1. The phosphorus Schiff base ligand was prepared by the condensation of Diphenyl chlorophosphate with the prepared Schiff base (SB) in the molar ratio 1:1 to form (OPSB). The ligand ratio of

(SB) with Cu(II), Ni(II) , and Co(II) complexes was found to be 1:2, and The ligand ratio of (OPSB) with Cu(II), Ni(II) , and Co(II) complexes was found to be 1:1 .

The ligands are insoluble in water but soluble in all organic solvents. All the synthesized complexes are stable, can be stored for long periods at room temperature, and are highly colored. The ligands are in soluble in water but soluble in the organic solvents. The complexes of SB are insoluble in water and common organic solvents but soluble in polar solvents such as DMF and DMSO. The complexes of OPSB are slightly soluble in water and soluble in common organic solvents. The molar conductance values in DMF for the complexes indicate that the complexes of SB are non-electrolytes [27,28] and the complexes of OPSB are of type 1:1 electrolytes in nature [27,29]. Two chloride ions were found in all the complexes of SB. They were found inside the coordination sphere by a simple silver nitrate test. No precipitation was first observed upon the addition of silver nitrate to the solution of the complexes. However, after digestion with nitric acid, the silver nitrate test gave a positive result suggesting the presence of the chloride ions. Concerning the complexes of OPSB, the precipitation was observed upon the addition of silver nitrate to the solution of the complexes [20].

Physical, elemental, spectral, and XRD data were listed in Tables 2-7 which agree with proposed structures (Figures 1 and 2).

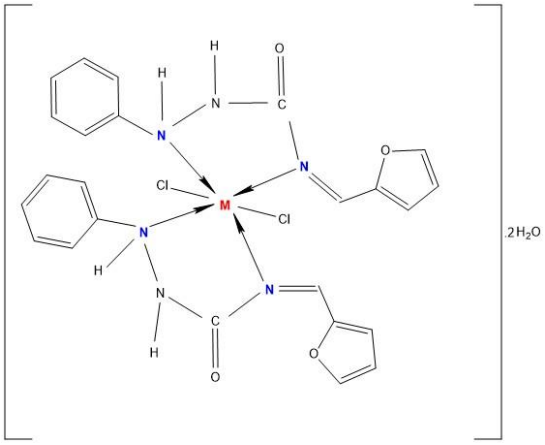

where M = Cu^{2+}, Ni^{2+} or Co^{2+}

Figure1 : Proposed structure of **SB** complexes

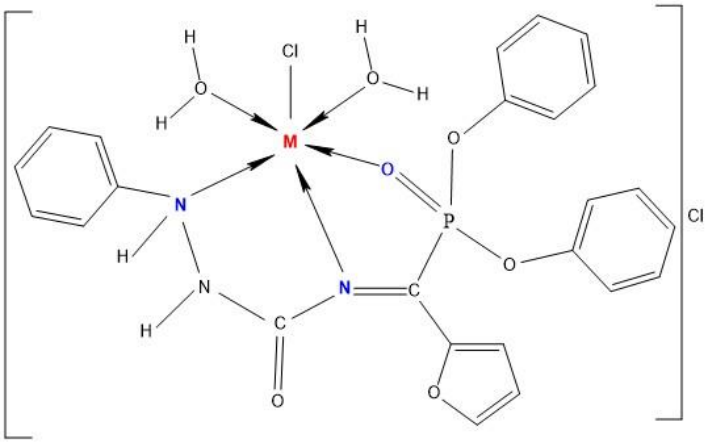

where M = Cu^{2+}, Ni^{2+} or Co^{2+}

Figure 2: Proposed structure of **OPSB** complexes

Table 2: Some physical properties and elemental analysis of the ligands and their complexes

Compound	Color (Yield)	M.P. (C^0)	Λm (Ω^{-1} cm^2 mol^{-1})	F. Wt. (g/mole)	Element Analysis Calculated% (Found)				
					C	H	N	P	M
$C_{12}H_{11}N_3O_2$(SB)	Gray 87%	177	-	229.24	62.87 (62.51)	5.22 (5.09)	18.33 (17.82)	-	-
$C_{23}H_{10}N_3O_5P$(OPSB)	brown 88%	148	-	439.32	62.88 (62.04)	2.29 (2.33)	9.56 (9.20)	7.05 (6.89)	-
$[Cu(SB)_2Cl_2].2H_2O$	Reddish brown 33%	140	11.90	628.96	45.83 (46.12)	4.16 (4.30)	13.36 (13.75)	-	10.10 (9.87)
$[Ni(SB)_2Cl_2].2H_2O$	Dark red 45%	270	9.14	624.11	46.18 (46.43)	4.20 (3.94)	13.46 (13.58)	-	9.40 (9.22)
$[Co(SB)_2Cl_2].2H_2O$	Brown 37%	175	14.61	624.35	46.16 (45.84)	4.19 (3.79)	13.44 (13.85)	-	9.43 (9.76)
$[Cu(OPSB)Cl.(H_2O)_2].Cl$	Dark brown 23%	160	70.95	609.80	45.30 (44.97)	2.31 (2.50)	6.89 (6.91)	5.07 (5.19)	10.42 (10.35)
$[Ni(OPSB)Cl.(H_2O)_2].Cl$	red 28%	108	80.75	604.95	45.66 (45.61)	2.33 (2.39)	6.95 (7.20)	5.12 (4.09)	9.70 (9.61)
$[Co(OPSB)Cl.(H_2O)_2].Cl$	Dark red 20%	112	76.72	605.19	45.64 (45.33)	2.33 (2.12)	6.94 (7.15)	5.11 (4.05)	9.30 (9.60)

3.1 Nuclear magnetic resonance spectral studies

3.1.1 ^{1}HNMR Spectra of the ligands

Figures (3 and 4) showed ^{1}HNMR spectra of the ligands SB and OPSB respectively. The azomethine proton appeared as a singlet signal at 7.947 ppm (s, 1H) in SB [30, 31] and this signal disappeared in the OPSB spectrum due to a replacement reaction on this group with eliminated HCl and forming P-C bond. The multiple signals around 6.752-7.670, and 6.711-7.592 ppm are ascribed to aromatic and furan ring protons of SB and OPSB respectively [32]. The peaks at 6.132, 6.726 and 5.972, 6.685 ppm were assigned to (N-H) groups in SB and OPSB respectively [29, 33].

3.1.2 ^{13}CNMR spectra of the ligands

Figures (5 and 6) showed ^{13}CNMR spectra of the ligands SB and OPSB respectively. They were characterized by the presence of a signal at 160.747 and 160.353 ppm of the carbonyl carbon C=O of SB and OPSB respectively [34,35]. Also, the spectra showed two peaks at δ 149.501 and δ149.630 ppm that attributed to azomethine carbon C=N [29]. The number of peaks between (112.265 - 129.164 and 112.174 129.051) ppm attributed to aromatic and furan ring carbon in SB and OPSB respectively [34,36].

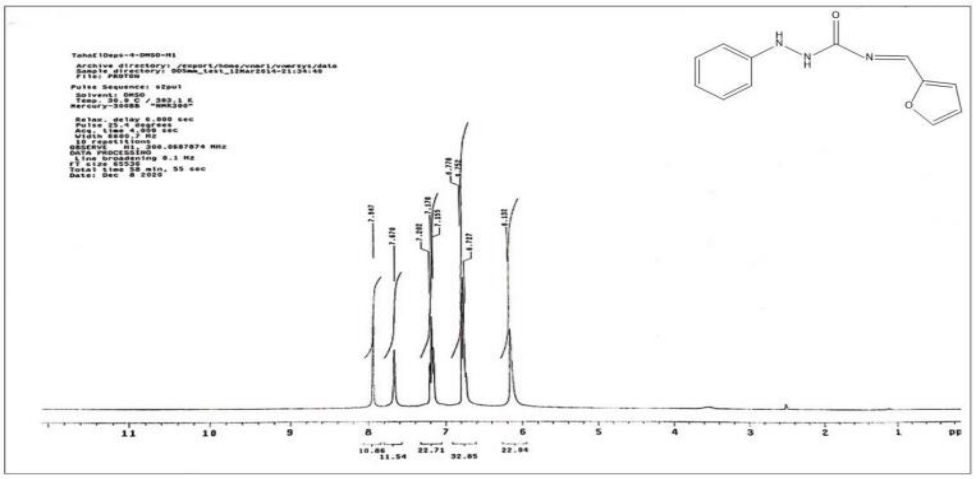

Figure 3: ^{1}HNMR spectrum of

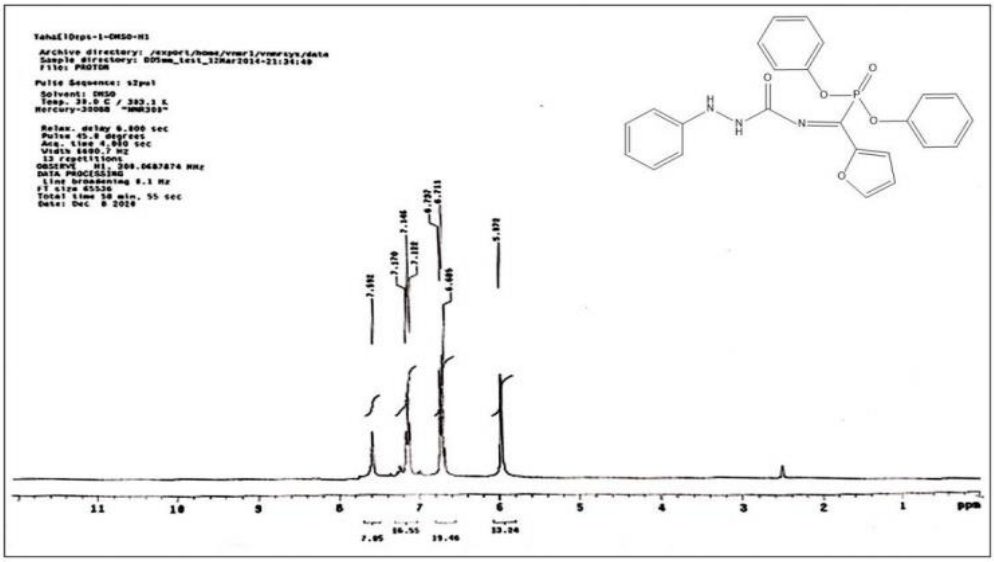

Figure 4: ^{1}HNMR spectrum of OPSB

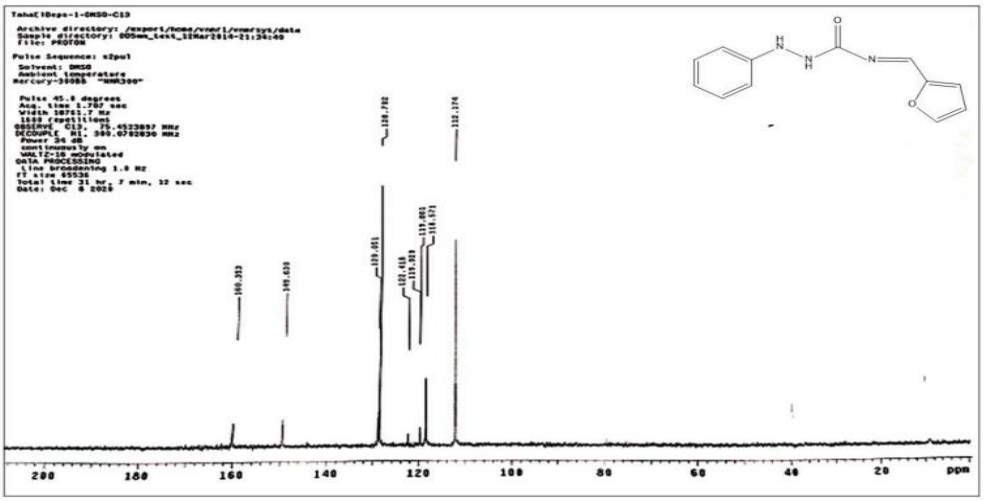

Figure 5: ^{13}CNMR spectrum of SB

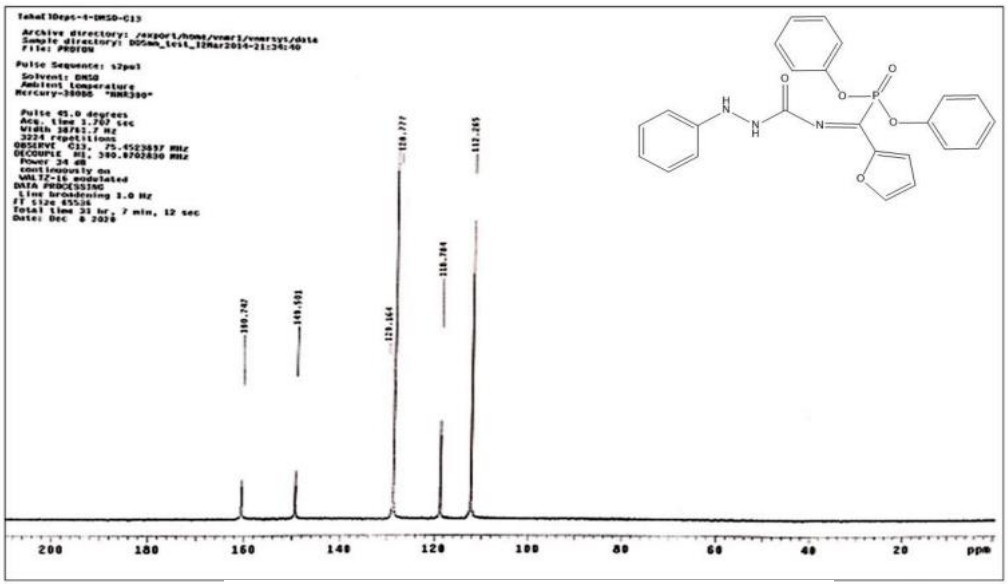

Figure 6: ^{13}CNMR spectrum of OPSB

3.2 Infra-red spectra of the ligands and their complexes

The main IR absorption bands of the ligands and their complexes are summarized in Table 3 and Figure 7. IR spectrum of ligand SB showed bands at 1656 cm^{-1} and 1600 cm^{-1} assigned to υ(C=O) and υ(C=N), respectively [37]. The strong bands of υ(NH) in this ligand were found at 3335 and 3398 cm-1 [38]. The bands were noticed at 3046 , 2928 and 1240 cm-1 that belong to of aromatic υ(C-H), aliphatic υ(C-H), and υ(-C-N) stretching modes of vibrations respectively [39].The band at 1505 cm-1 in its spectrum is able to be appointed to υ(C-O-C) of the furan ring [32].

The IR spectra of the metal complexes of ligand SB (Figure 7) have been studied in accord for the estimate of their structure. The shift of azomethine vibrations to the lower frequency indicates the coordination of nitrogen with metal ions. The bands of υ(NH,NH) disappeared in complexes due to the broad bands of water. New vibrations at 400-600 cm-1 that are not present in the free are attributed to the existence of υ(M-N) and υ(M-NH) [40]. The broad bands have been seen (3322-3423) cm-1 which correspond to the water molecules in the complexes formation [41]. All of these IR data confirm that a bidentate ligand is coordinated in Cu, Ni, and Co metal complexes.

Although the present evidence of υ(M-Cl) could not be brought in the IR data due to instrumental limitation, the insolubility of SB complexes in water and their non-electrolytic nature evinced that 2Cl- coordinated with metal in SB complexes.

In the ligand OPSB presence bands at 1662 cm-1and 1625 cm-1 that assigned to υ(C=O) and υ(C=N), respectively [37]. The IR spectrum (Figure 8) exhibited characteristic bands at 1191 cm-1 and 1082 cm-1 assigned to υ(P=O) and υ(P-O-C) respectively [15].

The bands between (3354-3386) cm-1 confirmed the presence of coordinated water with metal ions in Cu, Ni, and Co complexes respectively [28]. The IR spectra of the metal complexes of ligand OPSB (Figure 8) proposed that this ligand tridentate with the amine-nitrogen, azomethine-nitrogen , and phosphoryl-oxygen due The shift in the position of υ(NH), υ(P=O) and υ(C=N) (Table 3).

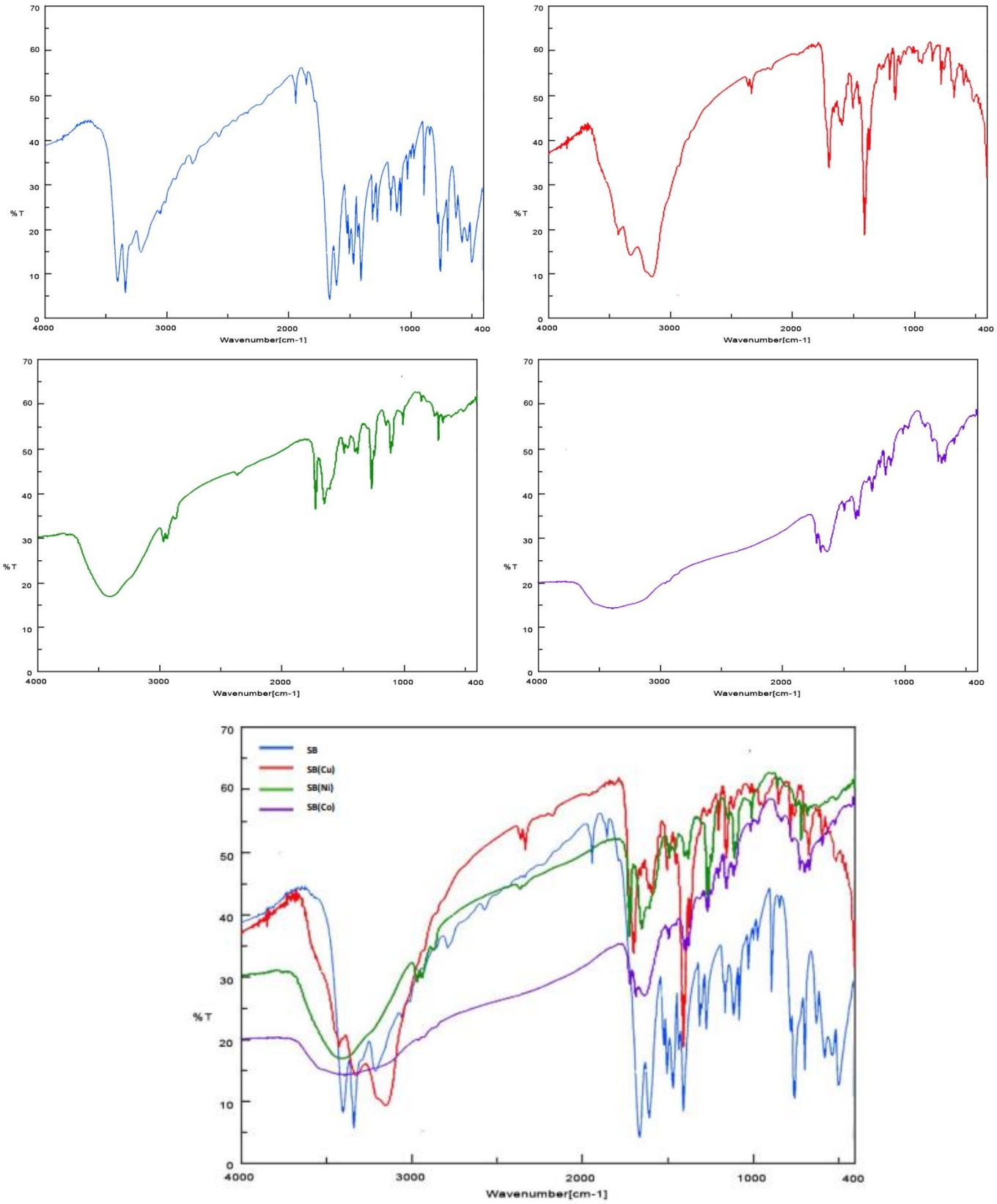

Figure 7: Infrared Spectra of SB and its complexes

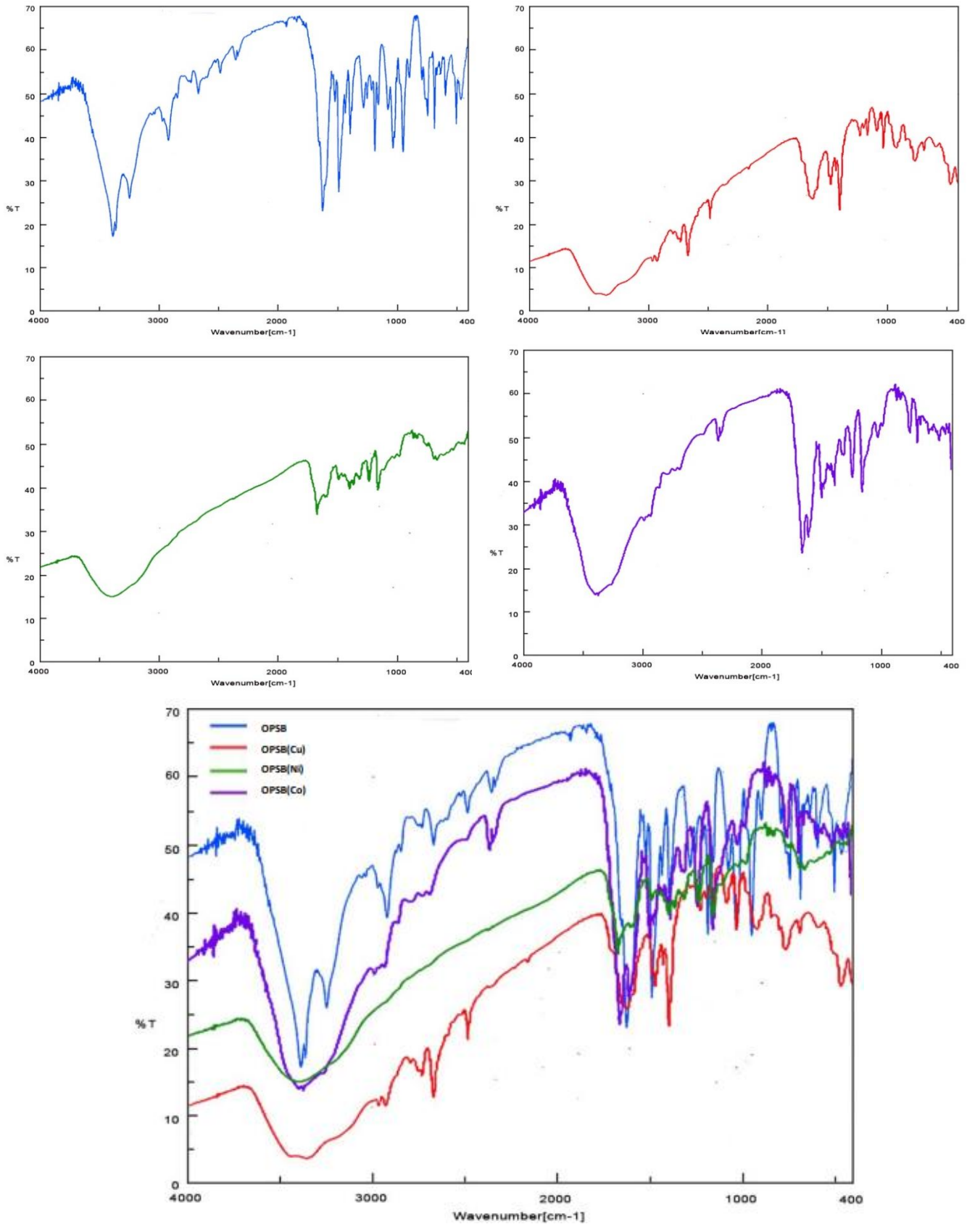

Figure 8: Infrared Spectra of OPSB and its complexes

3.3. Electronic spectra and magnetic measurements

Electronic spectral data and magnetic moments of the ligands and their complexes were presented in Table 4. The electronic absorption spectra were recorded in DMSO in the range 200 – 900 nm.

The electronic spectrum of SB (Figure 9) showed two bands at 35714.29 cm-1 of ($\pi \rightarrow \pi^*$) and 31250 cm-1 of ($n \rightarrow \pi^*$). Also, the electronic spectrum of OPSB (Figure 10) exhibited two bands at 37037.04 cm-1 of ($\pi \rightarrow \pi^*$) and 32258.06 cm-1 of ($n \rightarrow \pi^*$) transitions [42]. In the metal complexes of Cu(II), Ni(II), and Co(II) the bands of $n \rightarrow \pi^*$ transitions were shifted to a higher or lower wavelength upon ligands coordination with metals (Figure 9). These results due to the coordination between azomethine and amine groups with metals in SB and between azomethine amine, and phosphoryl groups.

The broad bands at 11904.76 and 13333.33 cm-1 in the Electronic spectra of the Cu(II) complexes with SB and OPSB (Figures 9,10) have been observed for the transition 2Eg→2T2g, the broadness of these bands is due to the Jahn-Teller effect [43]and the measured magnetic moment were 1.67 and 1.78. The octahedral geometry for Cu (II) complex has been suggested from these parameters [44].

In Ni(II) complexes with SB and OPSB (Figures 9,10), the bands were observed at (18867.92, 178571.42) and (20000-16393.44) cm-1 respectively, due to transitions 3A2g → 3T1g(P) and 3A2g → 3T1g(F) [43]. The two complexes are paramagnetic and measured magnetic moments are 2.77 and 2.89 which is compatible with these complexes having an octahedral structure [45].

The electronic spectra of Co(II) complexes with SB and OPSB (Figures 9,10) showed three bands at (20833.33, 19607.84, 16393.44) and (22727.27,1818.81,1515.51) cm-1 respectively, have been assigned to 4T1g→ 4T1g(P), 4T1g→ 4A2g and 4T1g→4T2g(F) transitions [44] and their magnetic susceptibilities are 4.66, 4.74B. M., respectively, this means the complexes have an octahedral structure [46].

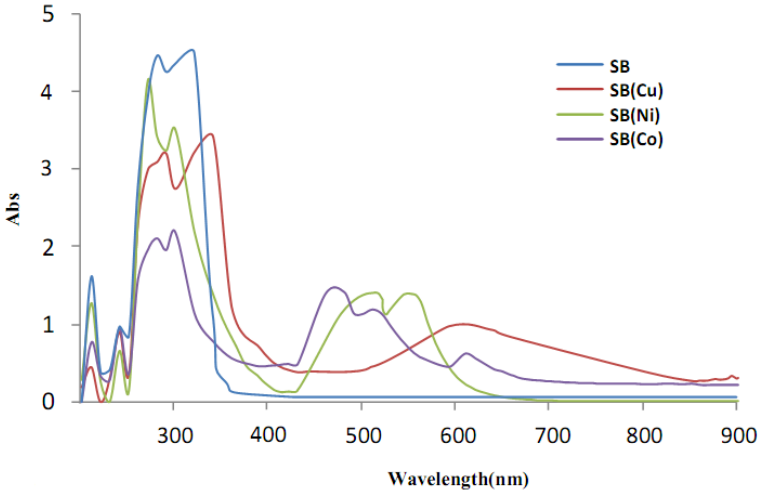

Figure 9: UV-Vis spectra of SB ligand and its complexes

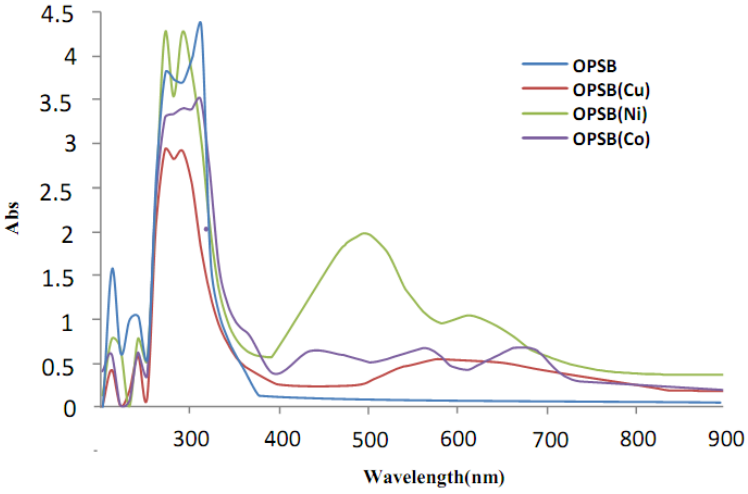

Figure 10: UV-Vis spectra of OPSB ligand and its complexes

Table 4: Electronic Spectral and Magnetic moment data of the ligands and their complexes

Compound	μeff (B.M.)	(*π→π) (n→π*) transition	d-d transition band (cm-1)	Assignments	Supposed structure
$C_{12}H_{11}N_3O_2$(SB)	-	35714.28 31250.00	-	-	-
$C_{23}H_{10}N_3O_5P$(OPSB)	-	37037.03 32258.06	-	-	-
$[Cu(SB)_2Cl_2].2H_2O$	1.67	34482.75 29411.76	11904.76	$^2Eg\rightarrow{}^2T_2g$	Distorted Octahedral
$[Ni(SB)_2Cl_2].2H_2O$	2.77	37037.03 34482.75	18867.92 178571.42	$^3A_2g \rightarrow {}^3T_1g(P)$ $^3A_2g \rightarrow {}^3T_1g(F)$	Octahedral
$[Co(SB)_2Cl_2].2H_2O$	4.66	35714.28 34482.75	20833.33 19607.84 16393.44	$^4T_1g\rightarrow {}^4T_1g(P)$ $^4T_1g\rightarrow {}^4A_2g$ $^4T_1g\rightarrow {}^4T_2g(F)$	Octahedral
$[Cu(OPSB)Cl.(H_2O)_2].Cl$	1.78	37037.03 34482.75	13333.33	$^2Eg\rightarrow{}^2T_2g$	Distorted Octahedral
$[Ni(OPSB)Cl.(H_2O)_2].Cl$	2.89	37037.03 34482.75	20000.00 16393.44	$^3A_2g \rightarrow {}^3T_1g(P)$ $^3A_2g \rightarrow {}^3T_1g(F)$	Octahedral
$[Co(OPSB)Cl.(H_2O)_2].Cl$	4.74	37037.03 33333.33	22727.27 1818.81 1515.51	$^4T_1g\rightarrow {}^4T_1g(P)$ $^4T_1g\rightarrow {}^4A_2g$ $^4T_1g\rightarrow {}^4T_2g(F)$	Octahedral

3.4. Molar ratio (stoichiometry) of the studied complexes

A study of the molecular structure of the complexes formed between the metal ions of (Cu^{2+}, $Ni^{2+,}$ and Co^{2+}) with ligands SB and OPSB in methanol using molar ratio detected the formation of SB complexes (2:1) (L:M) and (1:1) (L:M) for OPSB complexes. The results are depicted in Tables 5 ,6 and Figures 11,12.

Table 5: Molar ratios for determination of stoichiometry of the SB complexes in methanol

SB	Absorbance of complexes		
[L]/[M]	Cu(II)	Ni(II)	Co(II)
0.5:1	0.251	0.233	0.363
1:1	0.392	0.345	0.456
1.5:1	0.595	0.430	0.512
2:1	0.629	0.480	0.600
2.5:1	0.625	0.486	0.605
3:1	0.640	0.482	0.619
3.5:1	0.647	0.489	0.629
4:1	0.667	0.501	0.650

Table 6: Molar ratios for determination of stoichiometry of the OPSB complexes in methanol

OPSB	Absorbance of complexes		
[L]/[M]	Cu(II)	Ni(II)	Co(II)
0.25:1	0.075	0.111	0.047
0.5:1	0.102	0.156	0.079
0.75:1	0.134	0.200	0.123
1:1	0.171	0.225	0.163
1.25:1	0.180	0.220	0.165
1.5:1	0.189	0.218	0.162
1.75:1	0.191	0.223	0.164
2:1	0.195	0.221	0.165

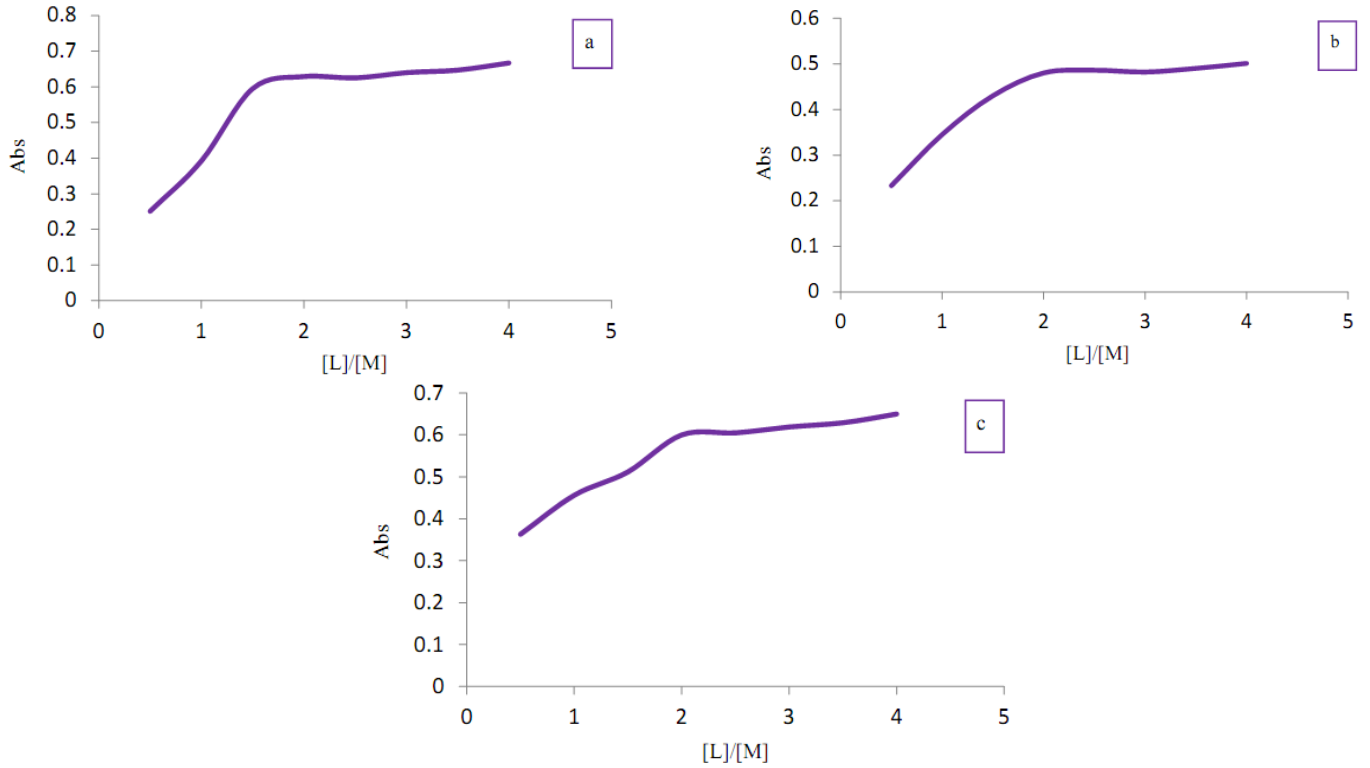

Figure 11: Molar ratio plot for the complexes between metal ions of (a)Cu, (b)Ni and (c)Co with SB in methanol

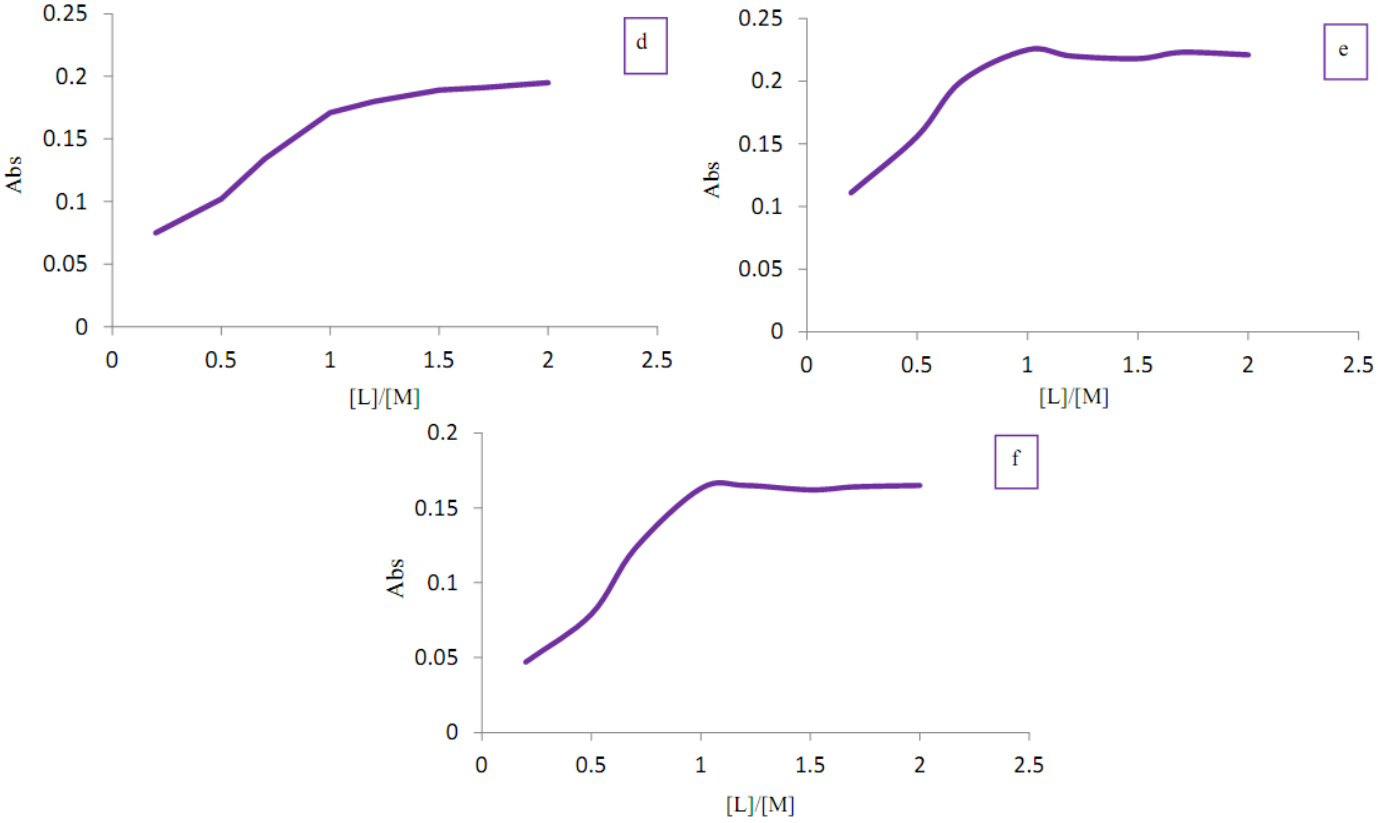

Figure 12: Molar ratio plot for the complexes between metal ions of (d)Cu, (e)Ni and (f)Co with OPSB in methanol

3.5 X-ray diffraction

Figures (13 – 16) represent the XRD patterns for SB and its complexes. From these Figures, a remarkable shift of the principal peak toward higher diffraction angles (Table 7) is observed for the complexes, suggesting the reduction of the unit cell dimensions and consequently contracting the crystal lattice [47]. In addition, the significant changes in intensities of the main peaks of SB complexes are observed in these figures attributed to the reduction in crystallinity. The crystallinity calculations are based on the ratio of the principal peaks area of the complex sample to that of the ligand sample obtaining a relative crystallinity [22]. The results in Table 7 show significant changes in crystallinity between SB and its complexes that exhibit low relative crystallinity (14.914%, 2.950%, 3.149%). In literature, the range between 1-100 nm is reported to be nanoparticle size [48]. so the particle size of the complexes obtained from XRD shows effects on their nanoparticle size (7.598 and 7.752 nm) due to complexation in case $[Cu(SB)_2Cl_2].2H_2O$ and $[Ni(SB)_2Cl_2].2H_2O$, but no change on nanoparticle size of $[Co(SB)_2Cl_2].2H_2O$.

Table 7: XRD spectra data of the principal values of intensity of the ligands and SB complexes

Compound	2θ	β	D (nm)	Mean D	X_C (%)
SB	7.141 14.120 16.001 19.300 20.700 22.560	0.226 0.439 0.221 0.369 0.632 0.290	6.419 3.323 6.616 3.980 2.329 5.091	4.626	100
OPSB	5.360 12.080 22.259 24.519	0.329 0.219 0.250 0.260	4.406 6.649 5.903 5.696	5.663	100
$[Cu(SB)_2Cl_2].2H_2O$	16.260 22.041 28.999 34.160	0.235 0.215 0.177 0.171	6.224 6.861 8.450 8.858	7.598	14.914
$[Ni(SB)_2Cl_2].2H_2O$	16.341 21.117 31.703 33.361	0.196 0.194 0.203 0.177	7.463 7.592 7.415 8.540	7.752	2.950
$[Co(SB)_2Cl_2].2H_2O$	16.620 18.639 20.940 31.700 33.561	0.633 0.255 0.272 0.293 0.290	2.311 5.754 5.413 5.137 5.215	4.766	3.149

About the OPSB ligand, its particle size was found within the nano range (5.663nm) (Table 7), nevertheless its complexes appeared as amorphous characters in figures (18 – 20). From this change, it is expected to improve the properties of OPSB complexes as compared with the OPSB ligand [49].

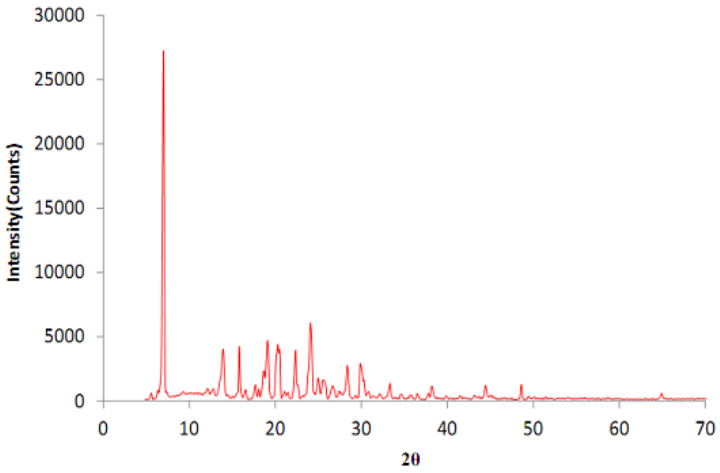

Figure 13: XRD pattern of SB

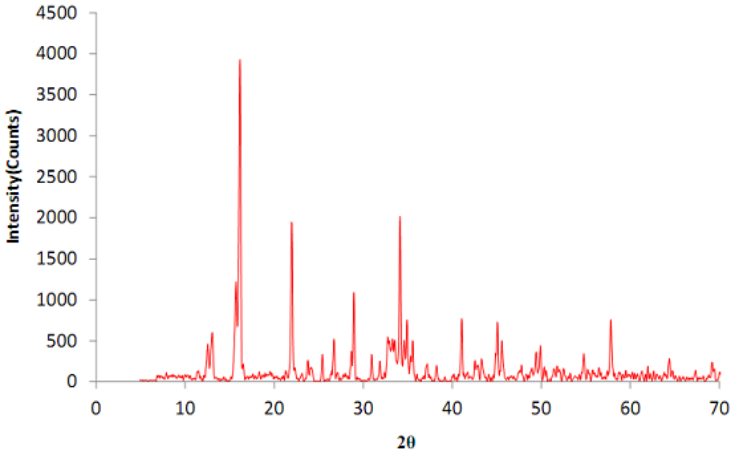

Figure 14: XRD pattern of SB(Cu)

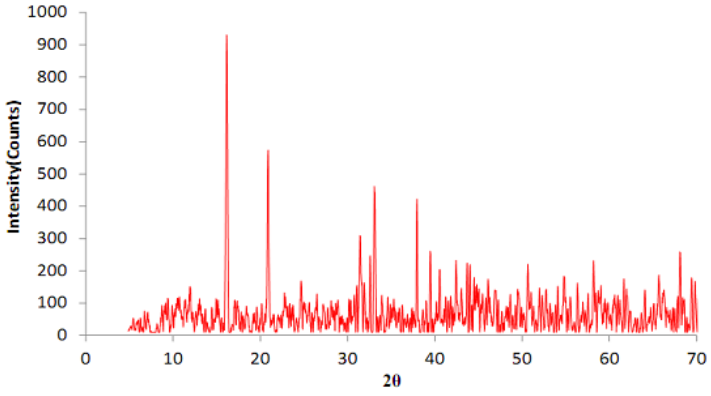

Figure 15: XRD pattern of SB(Ni)

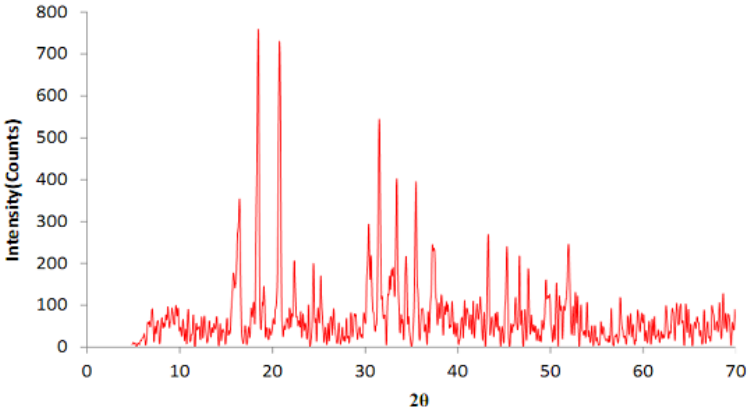

Figure 16: XRD pattern of SB(Co)

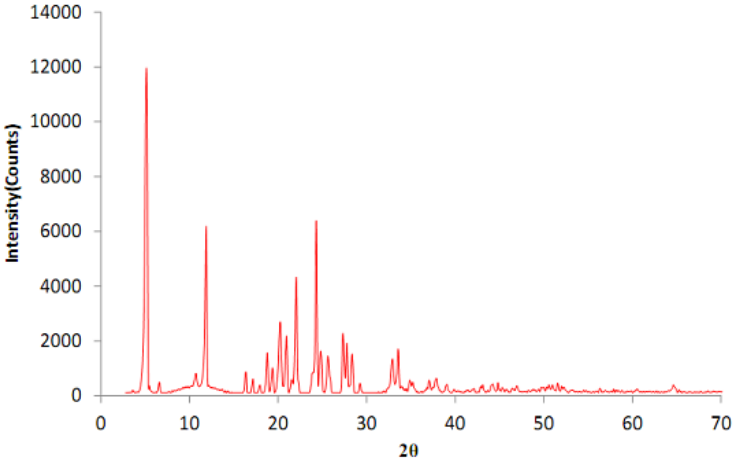

Figure 17: XRD pattern of OPSB

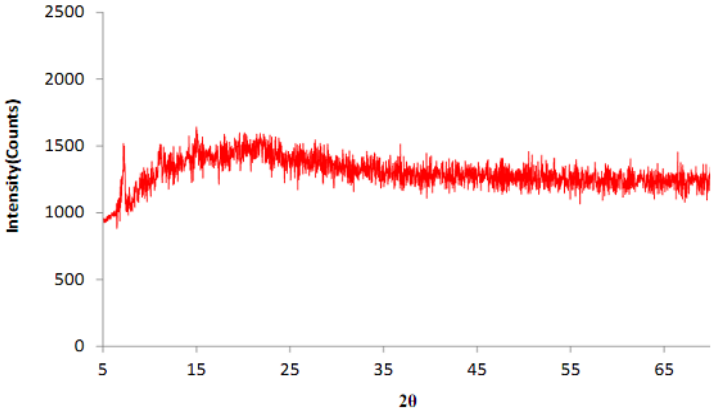

Figure 18: XRD pattern of OPSB(Cu)

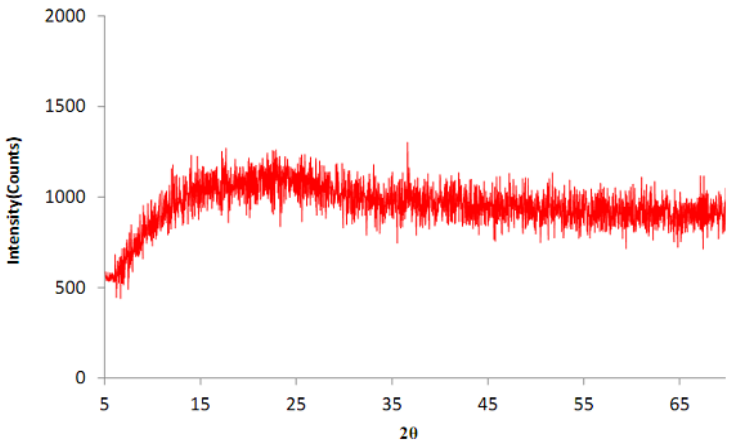

Figure 19: XRD pattern of OPSB(Ni)

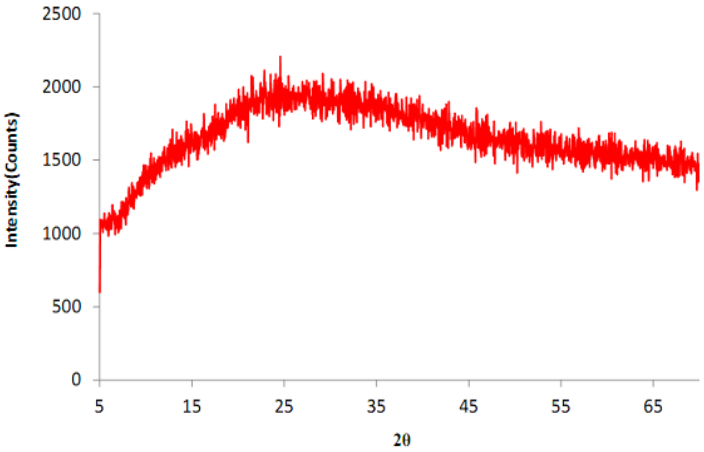

Figure 20: XRD pattern of OPSB(Co)

3.6 Antioxidant activity

The ligands and OPSB complexes were investigated using (FBRC) technique to determine the antioxidant activity [25]. It was taken (1 ml, 10-2 M FeCl3.6H2O) to a 10 ml volumetric flask different volumes of the standard antioxidants Ascorbic acid (0.1g/L) were added (0.01 ml, 0.02 ml, 0.04 ml, 0.06 ml, 0.08 ml, 0.1 ml, 0.2 ml). This was followed by 2.0 ml 0.3M acetate buffer (pH 4) and 1.0 ml bipyridine (6.4×10-3 M). The volume was completed to the mark with deionized water. After 10 min of incubation at room temperature, the absorbance was recorded against a blank at 535 nm. The absorbance values were plotted against the concentration of the various antioxidant solutions (Figure 21).

Similarly, 0.02 ml of (0.1mg/ml methanol) of each tested compound was reacted with 1 ml, 10-2 M FeCl3.6H2O solution, (6.4×10-3 M) bipyridine and 2.0 ml 0.3M acetate buffer (pH 4). This mixture was diluted to 10 ml with deionized water for the antioxidant assay.

Fe(II)-bipyridine complex produced by the reaction of Fe(III) with antioxidant followed by bipyridine exhibited maximum absorption at 535 nm (Scheme 3). Total antioxidant activity is based on the redox reaction between compounds and Fe(III) at room temperature. The initial antioxidant concentration is indicated by the concentration of the oxidizing Fe(III).

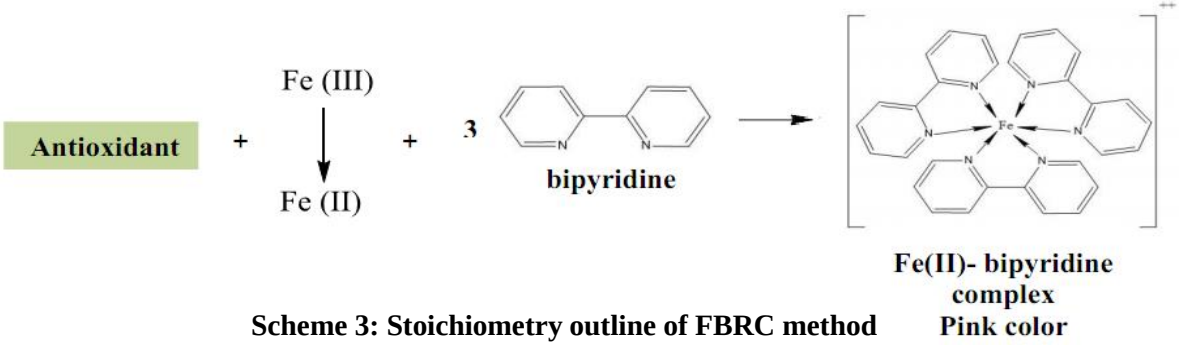

Scheme 3: Stoichiometry outline of FBRC method

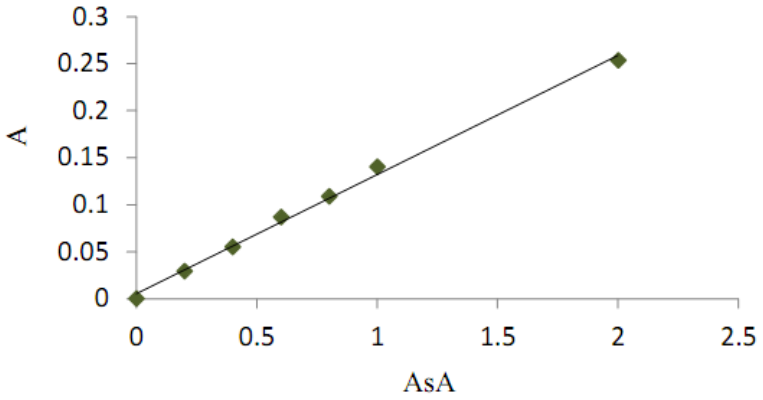

Figure 21: Calibration curve of ascorbic acid with Fe-Bp complex

Table 8: FBRC values express as (mg/L) for prepared compounds

sample	FBRC mg/L
SB	0.0223 ± 0.0002
OPSB	0.0218 ± 0.0002
[Cu(OPSB)Cl.$(H_2O)_2$].Cl	0.0188 ± 0.0001
[Ni(OPSB)Cl.$(H_2O)_2$].Cl	0.0176 ± 0.0003
[Co(OPSB)Cl.$(H_2O)_2$].Cl	0.0171 ± 0.0001

From the results in Table 8, we found that these compounds posse a potent antioxidant activity better than the standard antioxidant Ascorbic acid (vitamin C) due to the presence of a combination of donor sites such as amide oxygen and imine nitrogen [50].

3.7 Antibacterial and antifungal screening:

The ligands and their metal complexes have been screened for their antibacterial and antifungal activities using well diffusion method [23] against four types of Bacteria (*Staphylococcous aureus, Bacillus subtilis, Escherichia.Coli and Pseudomonas aeruginosa)* and one fungus (*Candida albicans*) on Nutrient agar and sabouraud agar solid media, respectively. The results obtained were presented in Table 9. From these results, it was observed that:

1- No inhibition zone was observed for ligands and their metal complexes against the fungus (*Candida albicans*).
2- The metal complexes are more potent bactericides than the ligands.
3- The Co(SB) complex exhibited higher antibacterial than the rest compounds except with *Escherichia.Coli*.

4- The order of antibacterial activity for the compounds with *Bacillus subtilis* was Co(SB) > Cu(SB) = Cu(OPSB) > OPSB > SB > Ni(SB) = Ni(OPSB) = Co(OPSB), with *Staphylococcous aureus* was Co(SB) > Co(OPSB) > Cu(SB) > Ni(OPSB) > SB = OPSB = Ni(SB) = Cu(OPSB), with *Escherichia.Coli* was Cu(OPSB) > Cu(SB) > Ni(OPSB) > Ni(SB) > SB = OPSB= Co(SB) = Co(OPSB) and with *Pseudomonas aeruginosa* was Co(SB) = Co(OPSB) > Ni(SB) > Cu(SB) > Cu(OPSB) > OPSB > SB> Ni(OPSB).

In general, the complexes showed good antibacterial compared to the free ligands. Based on the chelation theory [51], the increased inhibition activity of the metal complexes may be explained on the basis that their structures mainly possess C=N bonds. Besides, the coordination decreases the polarity of the metal ion due to the partial sharing of its positive charge with donor groups and possible π- electron delocalization inside the chelate ring-shaped during coordination that makes the complexes more lipophilic. This increased lipophilicity enhances the penetration of the metal complexes into lipid membranes, blocks the metal binding sites in the enzymes, and limits the further development of the organisms.

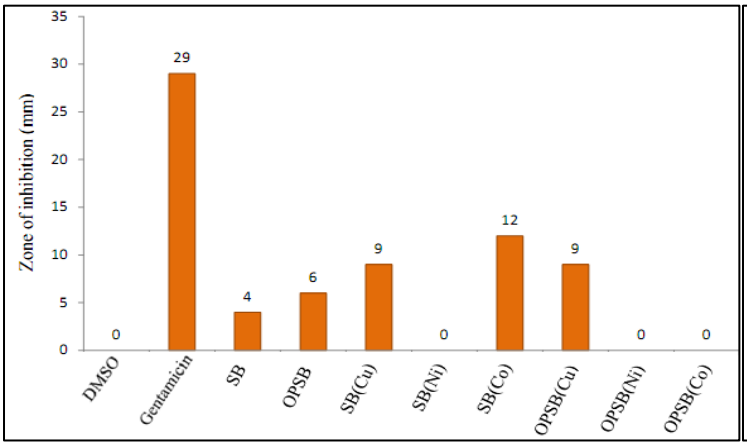

Figure 22: Antibacterial activity of the ligands and their metal complexes against gram-positive bacterium *Bacillus subtilis*

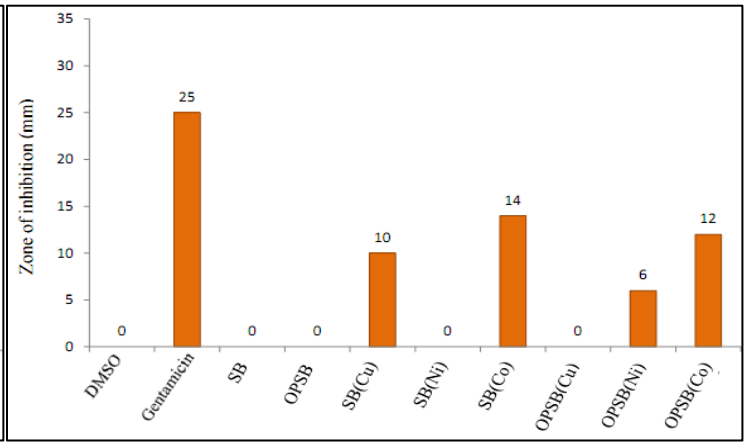

Figure 23: Antibacterial activity of the ligands and their metal complexes against gram-positive bacterium *Staphylococcus aureus*

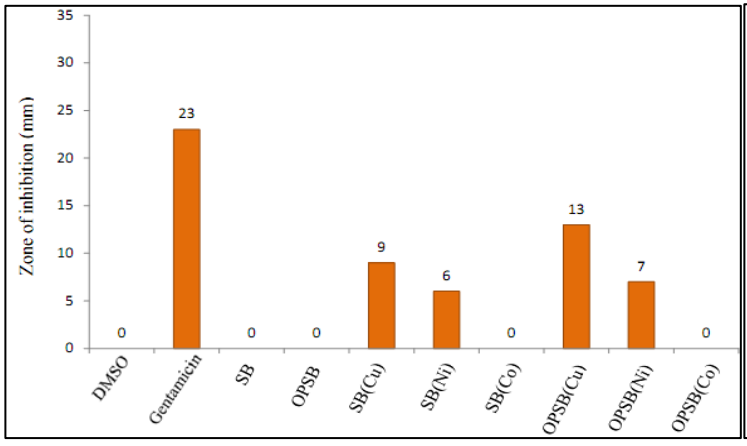

Figure 24: Antibacterial activity of the ligands and their metal complexes against gram-negative bacterium *Escherichia coli*

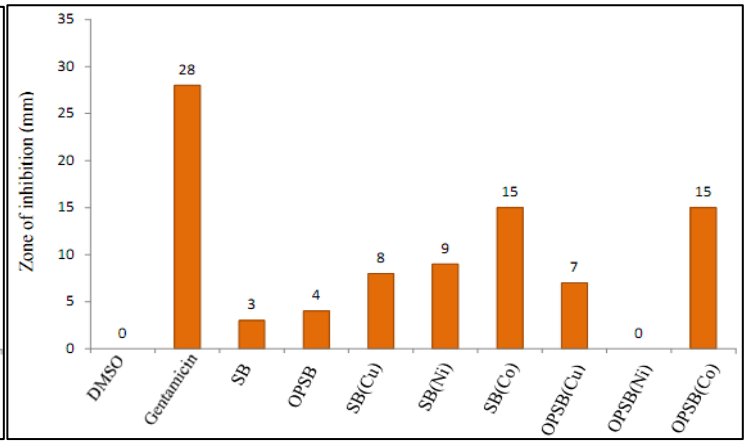

Figure 25: Antibacterial activity of the ligands and their metal complexes against gram-negative bacterium *Pseudomonas*

Table 9: Biological activities of the ligands and their metal complexes against bacteria and fungus (zone of inhibition in mm)

Compound (1000µg/ml)	Bacteria				Fungi
	gram-positive		gram-negative		
	Bacillus subtilis	*Staphylococcus aureus*	*Escherichia coli*	*Pseudomonas aeruginosa*	*Candida albicans*
SB	4	0	0	3	0
OPSB	6	0	0	4	0
$[Cu(SB)_2Cl_2].2H_2O$	9	10	9	8	0
$[Ni(SB)_2Cl_2].2H_2O$	0	0	6	9	0
$[Co(SB)_2Cl_2].2H_2O$	12	14	0	15	0
$[Cu(OPSB)Cl.(H_2O)_2].Cl$	9	0	13	7	0
$[Ni(OPSB)Cl.(H_2O)_2].Cl$	0	6	7	0	0
$[Co(OPSB)Cl.(H_2O)_2].Cl$	0	12	0	15	0
Gentamicin (120 µg/ml)	29	25	23	28	-
Mycostatin (30 µg/ml)	-	-	-	-	18

4. Conclusions

In the present study, we reported the preparation of new ligands (2-Furalidene-1-phenylsemicarbazide SB), (2-Furalidenediphenylphosphate-1-phenylsemicarbazide OPSB) and their metal complexes. These compounds were characterized by various spectral physicochemical methods. The UV-Vis, magnetic susceptibility results led to the conclusion that the metal complexes assumed the octahedral geometry via (NH) and (C=N) nitrogen in SB ligand, (NH), (C=N) nitrogen and P=O oxygen in OPSB ligand. remarkable changes of XRD patterns of the free ligands and their complexes were observed and the nature of crystanilly was observed with ligands and SB complexes, but in case the complex of OPSB showed amorphous nature. Ligands and OPSB complexes posed high antioxidant activity compared to standard antioxidant Ascorbic acid. The results of the antibacterial activity showed that, the complexes exhibited inhibition activity better than the ligands .

5. References

1- A. Abu-Yamin, M. S. Abduh, S. A. M. Saghir and N. Al-Gabri, Synthesis, Characterization and Biological Activities of New Schiff Base Compound and Its Lanthanide Complexes, Pharmaceuticals, 454 **(2022)** 1-15. https://doi.org/10.3390/ph15040454

2- G. G. Mohamed, M. M. Omar and Y. M. Ahmed, Metal complexes of Tridentate Schiff base : Synthesis, Characterization, Biological Activity and Molecular Docking Studies with COVID-19 Protein Receptor, Z. Anorg. Allg. Chem, 647 **(2021)** 2201–2222. https://doi.org/10.1002/zaac.202100245

3- R. Miri, N. Razzaghi-asl and M. K. Mohammadi, QM study and conformational analysis of an isatin Schiff base as a potential cytotoxic agent," Journal of Molecular Modeling, 19(2) **(2013)** 727–735. https://doi.org/10.1007/s00894-012-1586-x

4- X. Q. Song, Z. G. Wang, Y. Wang, Y. Y. Huang, Y.X. Sun, Y. Ouyang, C.Z. Xie and J.Y. Xu, Syntheses, characterization, DNA/HSA binding ability and antitumor activities of a family of isostructural binuclear lanthanide complexes containing hydrazine Schiff base. Journal of Biomolecular Structure and Dynamics. 38 (3) **(2020)** 733–743. https://doi.org/10.1080/07391102.2019.1587511

5- O. A. El-Gammal, F. S. Mohamed, G. N. Rezk and A. A. El-Bindary, Structural characterization and biological activity of a new metal complexes based of Schiff base. Journal of Molecular Liquids. 330 **(2021)** 115522. https://doi.org/10.1016/j.molliq.2021.115522

6- R. B. Aochar1, R. G. Mahale and R. S. Dhivare, synthesis, Physicochemical, Morphological and Antimicrobial Study of Schiff-Base Ligands Metal Complexe, Quest Journals, 8 (2) **(2022)** 01-06.

7- M. S. Suresh and V. Prakash, Preparation Characterization and Antibacterial Studies of Chelates of Schiff Base Derived from 4-Aminoantipyrine, Furfural and o-Phenylenediamine, E-Journal of Chemistry, 8(3) **(2011)** 1408-1416. https://doi.org/10.1155/2011/254018

8- L. John, R. S. Joseyphus and I. H. Joe, Biomedical application studies of Schif base metal complexes containing pyridine moiety: molecular docking and a DFT approach, SN Applied Sciences, 2 **(2020)** 500. https://doi.org/10.1007/s42452-020-2274-6

9- A. Prakash and S. Ahmad, Physico-chemical and antimicrobial studies on Ni(II), Cu (II) and Ti(III) Schiff base complexes derived from 2-furfuraldehyde, Oriental Journal of Chemistry, 25(2) **(2009)** 391-395.

10- R. K. Mohapatra, U. K. Mishra, S. K. Mishra, A. Mahapatra and D. C. Dash, Synthesis and Characterization of Transition Metal Complexes with Benzimidazolyl-2-hydrazones of o-anisaldehyde and Furfural, Journal of the Korean Chemical Society, 55(6) **(2011)** 926-931. https://doi.org/10.5012/jkcs.2011.55.6.926

11- Ö. Altun and M. Ö. Koçer, Pt(II) complex of Schiff base derived from L-phenylalanine and furfuraldehyde in the presence of 8-hydroxyquinoline: Structural analysis, composition of complex and biological activity, Comptes Rendus Chimie, 23(2) **(2020)** 127-142. https://doi.org/10.5802/crchim.9

12- Z.H. Abd El-Wahab and M.R. El-Sarrag, Derivatives of phosphate Schiff base transition metal complexes: synthesis, studies and biological activity, Spectrochimica Acta Part A, 60 **(2004)** 271–277. https://doi.org/10.1016/S1386-1425(03)00216-6
13- J. Ochocki, J. Graczyk and J. Reedijk, Synthesis and antitumor activity of novel Pt(II) diethyl pyridylmethylphosphonate complexes against sarcoma-180, Journal of Inorganic Biochemistry. 59 **(1995)** 240. https://doi.org/10.1016/0162-0134(95)97346-R
14- E. Brzezinska-Blaszezyk, M. Mincikiewicz and J. Ochocki, Effect of cisplatin and cis-platinum (II) phosphonate complex on murine mast cells. European Journal of Pharmacol. 298 **(1996)** 155. https://doi.org/ 10.1016/0014-2999(95)00809-8.
15- A. N. El-khazandar, ORGANO-PHOSPHORUS SCHIFF-BASES PART (IV): SYNTHESIS AND CHARACTERISTICS OF SOME PHOSPHATE SCHIFF-BASE COMPLEXES, Phosphorus, Sulfur, and Silicon and the Related Elements, 126 (1) **(1997)** 243-255. http://dx.doi.org/10.1080/10426509708043564
16- Z.H. Abd El-Wahab and M.R. El-Sarrag, Derivatives of phosphate Schiff base transition metal complexes: synthesis, studies and biological activity, Spectrochimica Acta Part A, 60 **(2004)** 271–277 http://dx.doi.org/10.1016/S1386-1425(03)00216-6
17- N. R.Bader, Sample preparation for flame atomic absorption spectroscopy: an overview, RJC, 4(1) (2011) 49-55.
18- M. R. Gaware, Study of electrical properties and solvent behaviour of 6-(4-Chlorophenyl)-1, 2, 3, 4-Tetrahydro-4-oxo-2-Thioxopyrimidine-5-carbonitrile at different temperatures,RJC,15 (1) (2022) 432-436. http://dx.doi.org/10.31788/RJC.2022.1516734
19- Z. Szafran, R. M. Pike, M. M. Singh, Microscale inorganic chemistry, J. Wiley, INC. New York (1991).
20- A.I. Vogel "A Text Book of Quantitative Inorganic Analysis" Longmans, London **(1961)**. https://books-library.net/files/books-library.online_nooc62bff6de966ff7ea138a8-34816.pdf
21- J.H.Yoe, A.L.Jones, Colorimetric Determination of Iron with Disodium-1,2-dihydroxybenzene-3,5-disulfonate, Ind.Eng.Chem.,Anel., Ed., 16(2) (1944) 111-115. https://pubs.acs.org/doi/abs/10.1021/i560126a015
22- B. Shah, V. K. Kakumanu and A. K. Bansal, Analytical techniques for quantification of amorphous/crystalline phases in pharmaceutical solids, J Pharm Sci., 95(8) **(2006)**1641-1665. https://doi.org/10.1002/jps.20644
23- A. Patterson, The Scherrer formula for X-ray particle size determination, Phys. Rev.,56 **(1939)** 978. https://doi.org/10.1103/PhysRev.56.978
24- M. Saeed, A. A. Alenad, M. A. Malik, Synthesis of mackinawite FeS thin films from acidic chemical baths, Materials Science in Semiconductor Processing, 32 **(2015)** 1-5. https://doi.org/10.1016/j.mssp.2014.12.073

25- K.M.Naji, F.H.Thamer, A.A.Numan, E.M.Dauqan, Y.M.Alshaibi, M.R. D'souza, Ferric-bipyridine assay: A novel spectrophotometric method for measurement of antioxidant capacity, Heliyon 6(1) **(2020)** 1-6. https://doi.org/10.1016/j.heliyon.2020.e03162
26- B. H. Ericsson, G. Tunevall and K. Wickman, The Paper Disc Method for Determination of Bacterial Sensitivity to Antibiotics: Relationship Between the Diameter of the Zone of Inhibition and the Minimum Inhibitory Concentration. Scandinavian Journal of Clinical and Laboratory Investigation, 12(4) **(1960)** 414-422. https://doi.org/10.3109/00365516009065406
27- W.J. Geary, The use of conductivity measurements in organic solvents for characterization of coordination compounds, Coordination Chemistry Review. 7(1) **(1971)** 18-122. https://doi.org/10.1016/S0010-8545(00)80009-0
28- A.O. Aderoju and M.W. Sherifah, Synthesis, characterization and antimicrobial activity of some mixed drug trimethoprim-sulfamethoxazole metal drug complexes, World Applied Journal, 33(2) **(2015)** 336-342. https://doi.org/10.5829/idosi.wasj.2015.33.02.22206
29- M. M. E. Shakdofa, A. N. Al-Hakimi, F. A. Elsaied, S. O. M. Alasbahi and A. M. A. Alkwlini, SYNTHESIS, CHARACTERIZATION AND BIOACTIVITY Zn^{2+}, Cu $^{2+}$, Ni^{2+}, Co^{2+}, Mn^{2+}, Fe^{3+}, Ru^{3+}, VO^{2+}, and UO^{2+} COMPLEXES OF 2-HYDROXY-5-((4-NITROPHENYL (DIAZENYL)BENZYLIDENE)-2-(p-TOLYLAMINO) ACETOHYDRAZIDE, Chemical Society of Ethiopia and The Authors, 31(1) **(2017)** 75-91. https://doi.org/10.4314/bcse.v31i1.7
30- C. Mohan , V.Kumar and S. Kumari, SYNTHESIS, CHARACTERIZATION, AND ANTIBACTERIAL ACTIVITY OF SCHIFF BASES DERIVED FROM THIOSEMICARBAZIDE, 2-ACETYL THIOPHENE AND THIOPHENE-2 ALDEHYDE, International Research Journal of Pharmacy, 9(7) **(2018)** 153-158. https://doi.org/10.7897/2230-8407.097141
31- P. Karuppusamy and S. Sarveswari, A simple diaminomaleonitrile based molecular probe for selective detection of Cu(II) and Zn(II) ions in semi-aqueous medium, Inorganica Chimica Acta, 515 **(2021)** 120073. https://doi.org/10.1016/j.ica.2020.120073
32- R. K. Mohapatra, U. K. Mishra, S. K. Mishra, A. Mahapatra and D. C. Dash, Synthesis and Characterization of Transition Metal Complexes with Benzimidazolyl-2-hydrazones of o-anisaldehyde and Furfural, Journal of the Korean Chemical Society, 55(6) **(2011)** 926- 931. https://doi.org/10.5012/jkcs.2011.55.6.926
33- A. S. EL-Tabl, F. A. EL-Saied and A. N. AL-Hakimi, Synthesis, spectroscopic investigation and biological activity of metal complexes with ONO trifunctionalalized hydrazone ligand, Transition Metal Chemistry, 32 (6) **(2007)** 689–701. http://dx.doi.org/10.1007/s11243-007-0228-0
34- M. S. Abdul Galil, A. N. Al-Hakimi, R. Y. Alshwafy, R. A.hmed Al Okab and A. Mutir, Synthesis, Structural Studies and Microbial Evaluation of Cu(II), Mn(II) Ni(II), Zn(II), Fe(III), Ru(III), VO(II), UO2(II) Complexes of Tetradentate Oxime-Hydrazon Ligand, Chemistry Journal, 1(3) **(2015)** 95-102. file:///C:/Users/96777/Downloads/70410015.pdf

35- F. Carrasco, W. Hern´andez, O. Chupayo, C. M. ´Alvarez, S. Oramas-Royo, E. Spodine, C. Tamariz-Angeles, P. Olivera-Gonzales and J. Z. D´avalos, Indole-3-carbaldehyde Semicarbazone Derivatives: Synthesis, Characterization and Antibacterial Activities, Hindawi Journal of Chemistry, **(2020)** 1-9. https://doi.org/10.1155/2020/7157281
36- A. A. Taqa, Some complexes of N-aryl furfural nitrones with Co (II), Ni (II), Cu (II), Zn (II) and Cd (II) chlorides, International Journal of Advanced Chemistry, 4 (1) **(2016)** 10-14. https://doi.org/10.14419/ijac.v4i1.6086
37- Md. S. Hossain, F. K. Camellia, N. Uddin, Md. Kudrat-E-Zahan, L. A. Banu, Md. M. Haque, Synthesis, Characterization and Antimicrobial Activity of Metal Complexes of N-(4-methoxybenzylidene) Isonicotinohydrazone Schiff Base, Asian Journal of Chemical Sciences, 6(1) **(2019)** 1-8. https://doi.org/10.9734/ajocs/2019/v6i118987
38- K. Nakamoto, Infrared and Raman Spectra of Inorganic and Coordination Compounds, Part A and Part B, John Wiley & Sons, New York, NY, USA, 1998.
39- A. M. Jassem, W. A. Radhi, H. A. Jaber and F. J. Mohammed, Synthesis and characterization of 1,3,4-Oxadiazoles Derivatives from 4-Phenyl-Semicarbazide, Journal of Basrah Researches Sciences, 39(3) **(2013)** 158-170. https://www.iasj.net/iasj/download/8d2c9cb3399655fa
40- S. K. Yassin, J. M. S. Alshawi and Z. A. M. Salih, Synthesis, characterization and cytotoxic activity study of Cu (II), Co (II), Mn (II), Ni (II) and Cr (III) Metal Complexes with new guanidine Schiff base against the hepatocellular Carcinoma (HCAM) cancer cell, Egyptian Journal of Chemistry, 63(10) **(2020)** 4005 – 4016. http://dx.doi.org/10.21608/EJCHEM.2020.37893.2778
41- C. González-García, A. Mata, F. Zani, M.A. Mendiola and E. López-Torres, Synthesis and antimicrobial activity of tetradentate ligands bearing hydrazone and/or thiosemicarbazone motifs and their diorganotin (IV) complexes, Journal of inorganic biochemistry, 163 (2016) 118-130. https://doi.org/10.1016/j.jinorgbio.2016.07.002
42- N.L. Mohammed, J.M.S. Al-Shawi, and M.J. Kadhim, Synthesis, Characterization and Thermal Studies of Schiff Bases Derived from 2,4-Dihydroxy benzaldehyde and their Complexes with Co(II), Ni (II), Cu(II), International Journal of Scientific Engineering and Research, 7(1) **(2019)** 31-40. https://www.ijser.in/archives/v7i1/IJSER18526.pdf
43- H.M. Al-Maydama, T.E.Y. Al-Ansi, Y.M. Jamil and A.H. Ali, Biheterocyclic ligands: synthesis, characterization and coordinating properties of bis(4-amino-5-mercapto-1,2,4-triazol-3-yl)alkanes with transition metal ions and their thermokinetic and biological studies, ECLETICA 33(3) **(2008)** 29-42. http://dx.doi.org/10.1590/S0100-46702008000300005
44- . Gup and B. Kirkan, Synthesis and spectroscopic studies of copper(II) and nickel(II) complexes containing hydrazonic ligands and heterocyclic coligand, Spectrochim. Acta Part A Mol. Biomol. Spectrosc, 62(4,5) **(2005)** 1188-1195. https://doi.org/10.1016/j.saa.2005.04.015
45- A. N. Al-Hakimi, M. M. E. Shakdofa, A. M. A. El-Seidy and A.S. El-Tabl, Synthesis, spectroscopic and biological studies of chromium(III), manganese(II), iron(III), cobalt(II), nickel(II), copper(II), ruthenium(III), and

zirconyl(II) complexes of N1,N2-bis(3-((3 -hydroxynaphthal en-2-yl)methylene-amino)propyl) phthalamide. J. Korean Chem. Soc., 55 **(2011)** 418-429.
https://doi.org/10.5012/JKCS.2011.55.3.418

46- M.F.R. Fouda, M.M. Abd-Elzaher, M.M. Shakdofa, F.A. El-Saied, M.I. Ayad and A.S. El Tabl, Synthesis and characterization of a hydrazone ligand containing antipyrine and its transition metal complexes. J. Coord. Chem., 61(12) **(2008)** 1983-1996.
https://doi.org/10.1080/00958970701795714

47- P. Barpanda, N. Recham, J. Chotard, K. Djellab, W. Walker,M. Armand and J. Tarascon, Structure and electrochemical properties of novel mixed Li(Fe1-xMx)SO_4F (M = Co, Ni, Mn) phases fabricated by low temperature ionothermal synthesis, Journal of Materials Chemistry, 20 **(2010)** 1659–1668.
https://doi.org/10.1039/b922063a

48- D. R. Boverhof, C. M. Bramante, J. H. Butala, S. F. Clancy, M. Lafranconi, J. West and S. C. Gordon, Comparative assessment of nanomaterial definitions and safety evaluation considerations, Regulatory Toxicology and Pharmacology, 73(1) **(2015)** 137-150.
https://doi.org/10.1016/j.yrtph.2015.06.001

49- M. S. Refat, F. M. Al-Azab, H. M. A. Al-Maydama, R. R. Amin, Y. M. S. Jamil, Preparation, spectroscopic and thermal characterization of new La(III), Ce(III), Sm(III) and Y(III) complexes of enalapril maleate drug. In vitro antimicrobial assessment studies, Journal of Molecular Structure, 1059 **(2014)** 208-224.
https://doi.org/10.1016/j.molstruc.2013.12.003

50- I. Kostova and L. Saso, Advances in Research of Schiff-Base Metal Complexes as Potent Antioxidants, Current Medicinal Chemistry, 20 (36) **(2013)** 4609-4632.
https://doi.org/10.2174/09298673113209990149

51- T.J. Franklin and G.A. Snow, Biochemistry of Antimicrobial Action, 4th[ed.], Chapman and Hall: London, **(1989)** 216.
https://www.academia.edu/36568156